Proceedings of the 9th World Congress on Mechanical, Chemical, and Material Engineering (MCM'23)
Brunel University, London, United Kingdom - August 06-08, 2023
Paper No. MMME 133
DOI: 10.11159/mmme23.133

Nuclear Radiation Shielding Capabilities Of Fiber-Reinforced Concrete: A Case Study Hybrid-Polypropylene-Steel

M. Ehab[1,*] and Ahmed Deifalla [2]
[1]Assistant Professor, Engineering Mathematics and Physics Department, Faculty of Engineering and Technology, Future University in Egypt, New Cairo 11835, Egypt. mehab@fue.edu.eg
[2]Professor, Structural engineering and Construction management department, Future University in Egypt, Cairo 11835, Egypt. ahmed.deifalla@fue.edu.eg
*Correspondence: mehab@fue.edu.eg

Abstract - As Fiber reinforced concrete (FRC) have superior properties over the conventional concrete; however, this superiority depends on the types of fiber used inside the concrete mixture. Radiation attenuation parameters as linear attenuation coefficient μ (LAC), mass attenuation coefficients μ_m (MAC), Half Value Layer (HVL), Tenth Value Layer (TVL) and Mean Free Path (MFP), were calculated for the studied Hybrid-Polypropylene-Steel, FRC, at photon energies 80, 356, 662 and 1333 KeV. For the findings of the study, the hybrid fiber-reinforced concrete is suitable for the nuclear shielding applications. In addition, the increase in the fiber contents improves the shielding efficiency.

Keywords: FRC; Radiation; Shielding; MAC; MFP

1. Introduction

Fiber reinforced concrete (FRC) containing several fiber types, namely hybrid FRC (HFRC), benefit greatly from the benefits of each fiber type. Fibers increase the concrete strength and delay the crack propagation [1]–[3]. The mechanical behavior of hybrid concrete using a mix of steel-polypropylene fiber has been investigated in previous studies [1-3]. In many applications concretes is exposed to radiation or elevated temperature[4].

By appropriately upholding the three fundamental principles of time, distance, and shielding, human exposure to external radiation from various sources can be reduced [5]–[8]. Reducing exposure time, increasing separation from the source, and using a shielding material can all minimize the radiation dose from external exposure. Due to the experimental conditions, reducing the exposure time might be challenging, but remote operation involves sophisticated instrumentation to monitor the operation. Utilizing an absorber, which decreases the radiation intensity and, as a result, its effective dose, is the most effective technique. Depending on radiation type, energy, temperature of the surrounding area, other considerations like space and economy, different types of shielding materials are implemented. [5], [7], [9]–[11].

A material's performance as a radiation shield is typically measured by its ability to prevent the incident radiation from penetrating through various kinds of interaction mechanisms. Gamma radiation is characterised by its strong penetration power. As it interacts with matter through three different processes: the photoelectric effect, Compton scattering, and pair production. [12]–[15]. The energy of the incident gamma radiation and the composition of the shielding material both affect how likely each interaction will be. The main mechanism through which low-energy gamma radiation interacts with materials having a high atomic number is photoelectric absorption, while pair production becomes the main process for high-energy gamma radiation [16], [17]. The linear attenuation coefficient (μ), which depends on both the energy of the incident radiation and the properties of the material, describes the bulk behavior of gamma interaction with the shield material [7], [8], [11], [15], [18]. The coefficient of mass attenuation (μ/ρ) of the photon was introduced to explain the properties of composite materials in terms of equivalent elements so that radiation in a tissue or equivalent material could be compared. [19].

Desirable shielding material has minimal effects on its mechanical, thermal, and electrical properties, as well as its chemical and physical stability, in addition to its ability to attenuate gamma radiation. Several factors, such as the type of radiation and its energy level, radiation intensity, material cost, and the variety of material attributes, such as weight, toxicity, and environmental compatibility, should all be taken into account while designing a radiation shield [5], [9]–[11], [18]. Frequently utilized materials for gamma radiation shielding are bismuth, lead, and concrete. Exploring the application of FRC in specialised concrete structures, such as nuclear power plants, is of tremendous interest. In these unusual applications, FRC will be subjected to gamma radiation[20]–[22]. There is little to no information in the public domain about how long FRCs can last when exposed to the conditions seen in nuclear power plants. [20], [23].

Thus, in the current study, various HFRC mixtures were tested for shielding properties. Concluding remarks were outlined and discussed.

2. Experimental Program

The experimental program investigated the shielding properties of hybrid-fibers high-strength concrete mixtures (flexural, tensile strength, and compressive strength) that were exposed to various photon energies.

2.1. Preparation of Specimens

The mix was prepared with the following components: cement, crushed granite, fine sand, and silica fume. Using the mechanical dry mixer for 2–3 min, components were dry mixed. Following that, wet mixing for 5 min along with 75% of the superplasticizer and all of the water, Then, the steel fiber and polypropylene fiber were slowly thrown into the mixture by hand and mixed thoroughly for another 3 min. Finally, the residual superplasticizer was added, and mixing was continued until a good flowability was produced. The mix quantities in weight-based for one cubic meter of fresh concrete for each admixture is as shown in Table 1 [1].

Table 1. Mix Properties [1].

Group	Mix	Polypropylene Fiber Volume (%)	Steel Fiber Volume (%)	Silica Fume (Kg/m3)	Cement (Kg/m3)	W/C Ratio	Coarse Agg. (Kg/m3)	Fine Agg. (Kg/m3)	Super Plasticizer (Lit./m3)
Control Mix	**M0/0**	-----	------	25	500	0.40	1148	705	6.4
G1	**M0/7**	-----	7	25	500	0.40	1148	705	6.4
	M0.3/7	0.3		25	500	0.40	1148	705	6.4
	M0.45/7	0.45		25	500	0.40	1148	705	6.4
	M0.6/7	0.6		25	500	0.40	1148	705	6.4

2.2 Calculation methods of shielding parameters:

The shielding effectiveness of materials can be examined on the basis of different parameters which include linear attenuation coefficient (μ), mass attenuation coefficient (μ_m), half value thickness (HVT), tenth value thickness (TVT),and mean free path (MFP) [18], [24].

A parallel beam of the measured intensity I of the transmitted mono-energetic X-ray or gamma-ray photons attenuated in the matter is related to the incident intensity I_0 is usually referred to as Beer-Lambert law is given by the relation [25]:

$$I = \boldsymbol{I_0 e^{-\mu t}} \quad (1)$$

Where $\boldsymbol{I_0}$ is the initial photon density, I is the photons that penetrate the alloy, μ is the total linear attenuation coefficient and t represents the thickness. By solving the Eq. (1), we get the equation for the linear attenuation coefficient μ ($\boldsymbol{cm^{-1}}$). The linear attenuation coefficient can be written as [18]:

$$\mu = \ln(\boldsymbol{I_0}/I) / t \quad (2)$$

The Mass Attenuation Coefficient $\mu_{\boldsymbol{m}}$ ($\mathbf{cm^2}$/g) for any mixtures of elements can be obtained by the following equation for a compound or mixture of elements [26], [27]:

$$\mu_{\boldsymbol{m}} = \mu/\rho \quad (3)$$

Where, ρ is the density of the constituent. The HVL and TVL are the thickness of an absorber sample that will reduce the initial radiation intensity to one-half and one-tenth, respectively. These can be calculated by [25], [28] :

$$HVL = Ln2 / \mu \quad (4)$$

, and

$$TVL = Ln10 / \mu \quad (5)$$

Mean free path is the average distance at which a single particle travels through the medium of given sample before interacting it with material and is calculated by the following equation [6], [18]:

$$MPF = 1/ \mu \quad (6)$$

3. Results and Discussion:

In this study, the protection rate against gamma radiation by Fiber-Reinforced Polymer (FRC) cubes was experimentally studied. For this purpose, Fiber-Reinforced Polymer (FRC) cubes, with thicknesses of 2, 4, and 6 cm were produced. In each thickness, samples (X1, X2, X3, and X4) were studied at 80, 356, 662, and 1333-keV photon energies. It was found that:

3.1 LAC:

Experimental linear attenuation coefficient μ ($\boldsymbol{cm^{-1}}$) for samples (X1, X2, X3, and X4) studied at 80, 356, 662, and 1333-keV gamma-ray energies, shown in Figure 1, decreases with the increasing of the photon energy for all of samples X1, X2, X3, and X4 for t=2,4, and 6 cm. It was also noted that with increasing thickness from t=2 to 6 cm, the linear attenuation slightly decreases, which means that increasing thickness does not have strong effect on LAC.

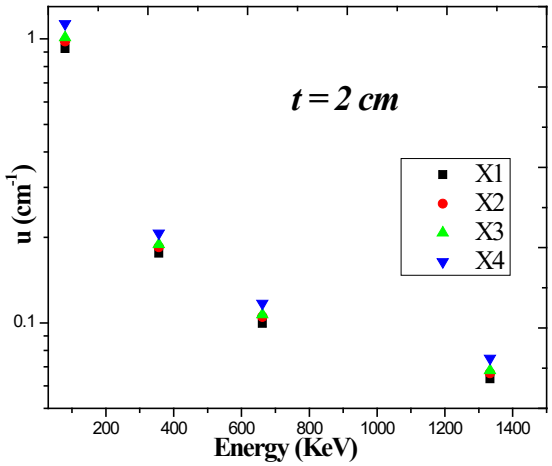

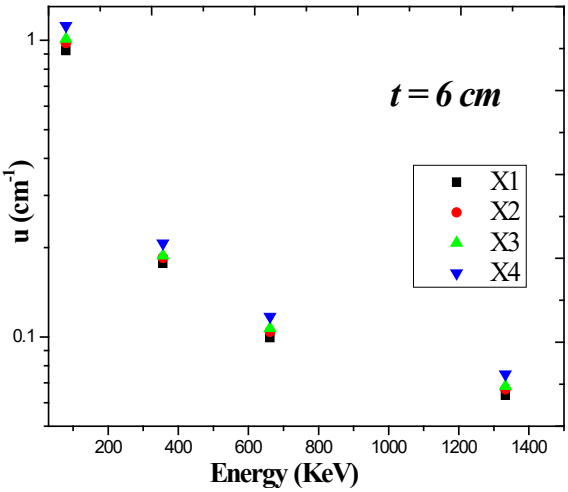

Fig. 1: Linear attenuation coefficients of the HFRC samples at different energies.

3.2 MAC:

As mass attenuation coefficient, μ_m ($\mu_m = \mu/\rho$) is of more vital importance than μ, it does not depend on the thickness and physical condition of the medium, so we choose thickness of 6 cm to calculate the relation between energy and MAC. Where the overall error in the measured (μ/ρ) is estimated to be ≤ 2% calculated from errors in intensities I_0 and I as there errors were estimated to be ≤ 1%. Mass attenuation coefficients μ_m (cm^2/g) for samples (X1, X2, X3, and X4) at thickness t= 6 cm, shown in Figure 2, illustrated the variation of μ_m of the prepared HFRC system with photon energy range from 80 to 1333 KeV that decreased with increasing energies increase. Based on the composition and photon energy, the obtained μ_m of the HFRC samples at same photon energy increases dramatically. The inverse proportion of μ_m of all samples with the energy increase is fundamentally well known due to the interaction of gamma energy with the material [29]. Distinguished variations of μ_m of the glass samples at low energy photon from 80, 356, and 662 KeV and at very high photon energy at 1333 KeV are obtained where photoelectric interaction and pair production are the most predominant interactions, respectively. The intermediate energy region from 662–1333 KeV is characterized by mass attenuation energy independent region where Compton interaction is dominant.

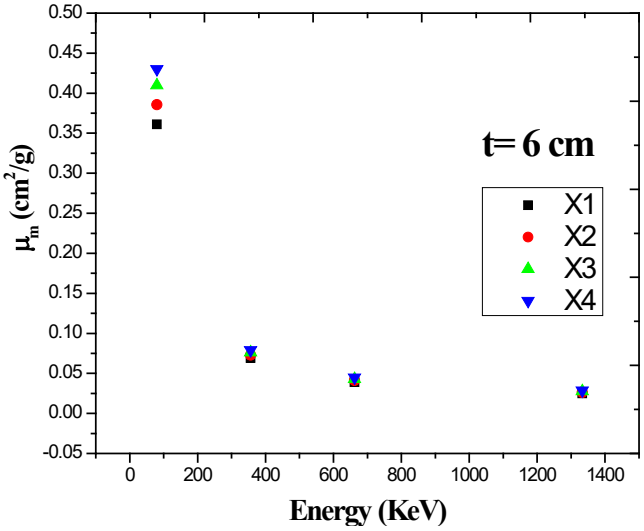

Fig. 2: Mass attenuation coefficients of HFRC samples at different energies at thicknesses of 6 cm

3.3 HVL and TVL:

Figure 3 illustrates increasing of Half Value Layer (HVL), and Tenth Value Layer (TVL) of the HFRC samples at same photon energy increases, where increasing the penetrating energy of a photon stream results in an increase in the HVL and TVL of a substance.

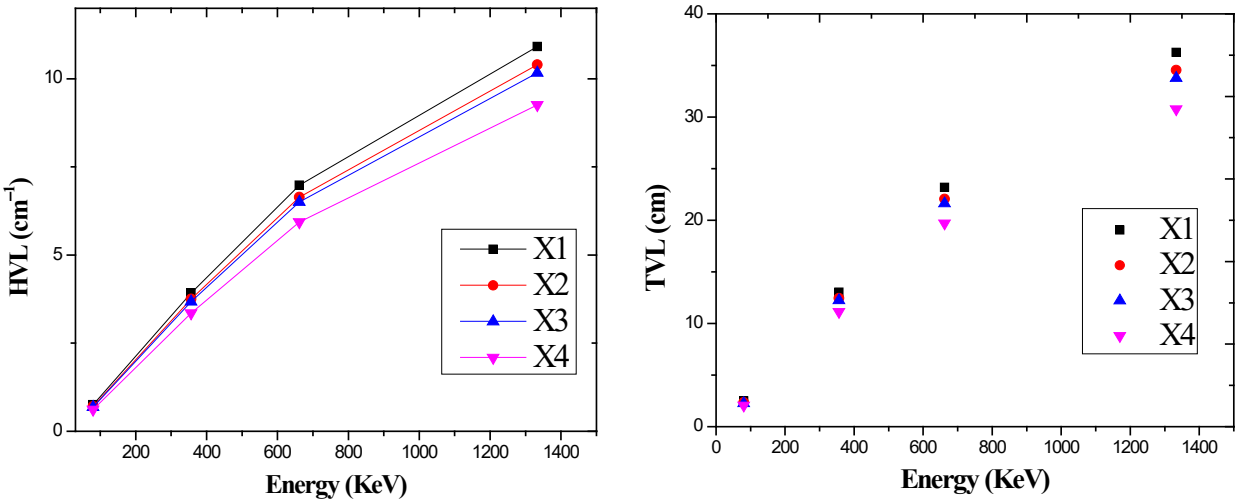

Fig. 3: The Half Value Layer (HVL) and The Tenth Value Layer (TVL) of the HFRC studied samples

3.4 MFP:

The Mean Free Path (MFP) describes the interaction of radiation with the shielding material atoms. Figure 4 shows that the HFRC samples at thickness t = 6 cm same photon energy increases with increasing energy.

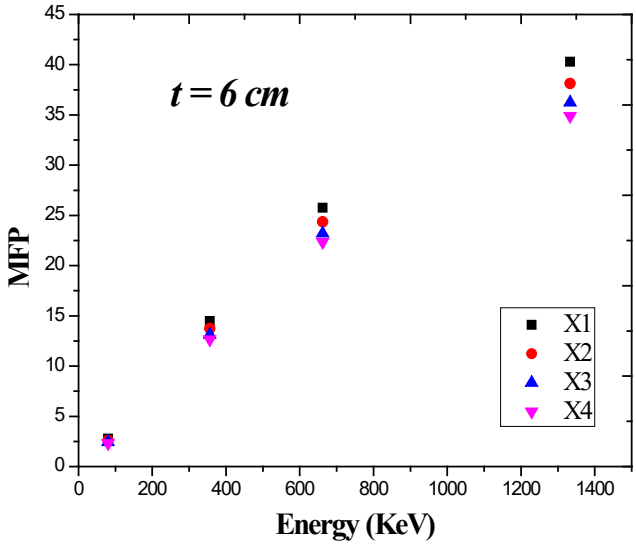

Fig. 4: The Mean Free Path (MFP) of all HFRC studied samples with energy at thickness t= 6 cm.

5. Conclusions:

The aim of this study is to investigate the radiation shielding characteristics of hybrid polypropylene-steel fiber-reinforced high-strength concrete to radiation shielding characteristics. The experimental study of this work can lead to the following reasonable conclusions:

1. Both LAC and MAC decrease with increasing energy.
2. Both HVL and TVL increase with increasing energies.
3. MFP increases with increasing energy.

The obtained radiation attenuation parameters results could nominate the prepared samples for various shielding applications. The increase in the fiber contents improves the shielding efficiency.

Acknowledgments: The authors would like to acknowledge the contribution of VELOCIT company and EDARA company from Egypt for donating steel fiber and polypropylene fiber. Also, The Future University in Egypt (FUE) for its Support and encouraging.

References:

[1] M. Tawfik, A. El-Said, A. Deifalla, and A. Awad, "Mechanical Properties of Hybrid Steel-Polypropylene Fiber Reinforced High Strength Concrete Exposed to Various Temperatures," *Fibers*, vol. 10, no. 6, 2022, doi: 10.3390/fib10060053.

[2] M. Gasser, O. Mahmoud, and A. Deifalla, "Reliable Machine Learning Model for Shear Strength of Reinforced Concrete Beams Strengthened Using FRP Jackets," no. May, 2022, doi: 10.20944/preprints202205.0170.v1.

[3] A. F. Deifalla, A. G. Zapris, and C. E. Chalioris, "Multivariable regression strength model for steel fiber-reinforced concrete beams under torsion," *Materials (Basel).*, vol. 14, no. 14, pp. 1–24, 2021, doi: 10.3390/ma14143889.

[4] H. Mohammed, H. Ahmed, R. Kurda, R. Alyousef, and A. F. Deifalla, "Heat-Induced Spalling of Concrete: A Review of the Influencing Factors and Their Importance to the Phenomenon," *Materials (Basel).*, vol. 15, no. 5, 2022, doi: 10.3390/ma15051693.

[5] I. Gaafar, A. El-Shershaby, I. Zeidan, and L. S. El-Ahll, "Natural radioactivity and radiation hazard assessment of phosphate mining, Quseir-Safaga area, Central Eastern Desert, Egypt," *NRIAG J. Astron. Geophys.*, vol. 5, no. 1, pp. 160–172, 2016, doi: 10.1016/j.nrjag.2016.02.002.

[6] S. Kaewjaeng, K. Boonyu, H. J. Kim, J. Kaewkhao, and S. Kothan, "Study on radiation shielding properties of glass samples doped with holmium," *AIP Conf. Proc.*, vol. 2279, no. October, 2020, doi: 10.1063/5.0022961.

[7] M. Ehab, S. U. El-kameesy, and E. Salama, "Indoor Radon Monitoring and Gamma Activity Levels Inside Some Ancient Egyptian Tombs in Luxor Indoor Radon Monitoring and Gamma Activity Levels Inside Some Ancient Egyptian," no. June, 2015, doi: 10.7324/IJASRE.

[8] S. U. El-Kameesy, E. Salama, S. A. El-fiki, M. Ehab, and W. Rühm, "Radiological safety assessment inside ancient Egyptian tombs in Saqqara," *Isotopes Environ. Health Stud.*, vol. 52, no. 6, pp. 567–576, 2016, doi: 10.1080/10256016.2016.1142444.

[9] I. Gaafar, M. Hanfi, L. S. El-Ahll, and I. Zeidan, "Assessment of radiation hazards from phosphate rocks, Sibaiya area, central eastern desert, Egypt," *Appl. Radiat. Isot.*, vol. 173, no. February, p. 109734, 2021, doi: 10.1016/j.apradiso.2021.109734.

[10] H. A. Esawii, E. Salama, L. Sayed El-ahll, M. Moustafa, and H. M. Saleh, "High impact tungsten-doped borosilicate glass composite for gamma and neutron transparent radiation shielding," *Prog. Nucl. Energy*, vol. 150, no. May, p. 104321, 2022, doi: 10.1016/j.pnucene.2022.104321.

[11] R. Gamal, E. Salama, M. Ehab, D. E. El-Nashar, and A. Bakry, "The effect of Gamma irradiation on the mechanical properties of Lead/SBR-NBR rubber blend," *AIP Conf. Proc.*, vol. 2620, no. June, 2023, doi:

10.1063/5.0120701.
[12] H. S. Husain, N. A. Rasheed Naji, and B. M. Mahmood, “Investigation of Gamma Ray Shielding by Polymer Composites,” *IOP Conf. Ser. Mater. Sci. Eng.*, vol. 454, no. 1, 2018, doi: 10.1088/1757-899X/454/1/012131.
[13] B. Aygün, “High alloyed new stainless steel shielding material for gamma and fast neutron radiation,” *Nucl. Eng. Technol.*, vol. 52, no. 3, pp. 647–653, 2020, doi: 10.1016/j.net.2019.08.017.
[14] H. S. Gökçe, Ç. Yalçınkaya, and M. Tuyan, “Optimization of reactive powder concrete by means of barite aggregate for both neutrons and gamma rays,” *Constr. Build. Mater.*, 2018, doi: 10.1016/j.conbuildmat.2018.09.022.
[15] M. Ehab, E. Salama, A. Ashour, M. Attallah, and H. M. Saleh, “Optical Properties and Gamma Radiation Shielding Capability of Transparent Barium Borosilicate Glass Composite,” *Sustain.*, vol. 14, no. 20, pp. 1–17, 2022, doi: 10.3390/su142013298.
[16] K. A. Mahmoud, E. Lacomme, M. I. Sayyed, F. Özpolat, and O. L. Tashlykov, “Investigation of the gamma ray shielding properties for polyvinyl chloride reinforced with chalcocite and hematite minerals,” *Heliyon*, vol. 6, no. 3, pp. 0–7, 2020, doi: 10.1016/j.heliyon.2020.e03560.
[17] A. M. Abu El-Soad, M. I. Sayyed, K. A. Mahmoud, E. Şakar, and E. G. Kovaleva, “Simulation studies for gamma ray shielding properties of Halloysite nanotubes using MCNP-5 code,” *Appl. Radiat. Isot.*, vol. 154, no. July, pp. 1–6, 2019, doi: 10.1016/j.apradiso.2019.108882.
[18] L. Sayed El-Ahll, E. Salama, H. A. Saudi, H. A. Alazab, and H. A. A. Ghany, “The Effect of Barium on the Nuclear Radiation Shielding Capabilities of Nickel-Reinforced Borosilicate Glasses,” *Silicon*, no. 0123456789, 2022, doi: 10.1007/s12633-021-01590-7.
[19] M. A. F. Zenobio, E. G. Zenobio, T. Augusto da Silva, and M. do Socorro Nogueira, “Mass attenuation coefficient (μ/ρ), effective atomic number (Z eff) and measurement of x-ray energy spectra using based calcium phosphate biomaterials: a comparative study,” no. 565, pp. 565–578, 2015.
[20] S. M. Homam and S. A. Sheikh, “Fiber-Reinforced Polymers Exposed to Nuclear Power Plant Environment,” *J. Compos. Constr.*, vol. 17, no. 6, p. 04013007, 2013, doi: 10.1061/(asce)cc.1943-5614.0000396.
[21] N. J. Abualroos and R. Zainon, “Fabrication of new non-hazardous tungsten carbide epoxy resin bricks for low energy gamma shielding in nuclear medicine,” *J. Phys. Commun.*, vol. 5, no. 9, 2021, doi: 10.1088/2399-6528/AC26DE.
[22] S. Thakur, V. Thakur, A. Kaur, and L. Singh, “Structural, optical and thermal properties of nickel doped bismuth borate glasses,” *J. Non. Cryst. Solids*, vol. 512, no. January, pp. 60–71, 2019, doi: 10.1016/j.jnoncrysol.2019.02.012.
[23] R. A. Abu Saleem, N. Abdelal, A. Alsabbagh, M. Al-Jarrah, and F. Al-Jawarneh, “Radiation shielding of fiber reinforced polymer composites incorporating lead nanoparticles—an empirical approach,” *Polymers (Basel).*, vol. 13, no. 21, pp. 1–15, 2021, doi: 10.3390/polym13213699.
[24] T. Singh, A. Kaur, J. Sharma, and P. S. Singh, “Gamma rays’ shielding parameters for some Pb-Cu binary alloys,” *Eng. Sci. Technol. an Int. J.*, vol. 21, no. 5, pp. 1078–1085, 2018, doi: 10.1016/j.jestch.2018.06.012.
[25] P. S. DAHINDE, G. P. DAPKE, S. D. RAUT, R. R. BHOSALE, and P. P. PAWAR, “ANALYSIS OF HALF VALUE LAYER (HVL), TENTH VALUE LAYER (TVL) AND MEAN FREE PATH (MFP) OF SOME OXIDES IN THE ENERGY RANGE OF 122KeV to 1330KeV,” *Indian J. Sci. Res.*, vol. 9, no. 2, pp. 79–84, 2019, doi: 10.32606/ijsr.v9.i2.00014.
[26] R. D. Iacobucci, S. A. Sheikh, and O. Bayrak, “Retrofit of Square Concrete Columns with Carbon Fiber-Reinforced Polymer for Seismic Resistance,” *ACI Struct. J.*, vol. 100, no. 6, pp. 785–794, 2003, doi: 10.14359/12845.

[27] E. RAJASEKHAR and R. JEEVAN KUMAR, “Experimental Investigation of Gamma Radiation Shielding Characteristics of Wood,” *BEST Int. J. Humanit. Arts, Med. Sci. (BEST IJHAMS)*, vol. 2, no. 6, pp. 21–26, 2014, [Online]. Available: http://www.bestjournals.in/view_archives.php?year=2014_73_2&id=73&jtype=2&page=3

[28] A. Akkaş, “Determination of the tenth and half value layer thickness of concretes with different densities,” *Acta Phys. Pol. A*, vol. 129, no. 4, pp. 770–772, 2016, doi: 10.12693/APhysPolA.129.770.

[29] E. Salama, A. Maher, and G. M. Youssef, “Gamma radiation and neutron shielding properties of transparent alkali borosilicate glass containing lead,” *J. Phys. Chem. Solids*, vol. 131, no. April, pp. 139–147, 2019, doi: 10.1016/j.jpcs.2019.04.002.